

# Chromophore Incorporation, $P_r$ to $P_{fr}$ Kinetics, and $P_{fr}$ Thermal Reversion of Recombinant N-Terminal Fragments of Phytochrome A and B Chromoproteins<sup>‡</sup>

Anja Remberg, Antje Ruddat, Silvia E. Braslavsky, Wolfgang Gärtner,\* and Kurt Schaffner

Max-Planck-Institut für Strahlenchemie, P.O. Box 101365, D-45413 Mülheim an der Ruhr, Germany

Received March 13, 1998; Revised Manuscript Received May 13, 1998

**ABSTRACT:** N-Terminal apoprotein fragments of oat phytochrome A (phyA) of 65 kDa (amino acids 1–595) and potato phyB of 66 kDa (1–596) were heterologously expressed in *Escherichia coli* and in the yeasts *Saccharomyces cerevisiae* and *Pichia pastoris*, and assembled with phytochromobilin (PΦB; native chromophore) and phycocyanobilin (PCB). The phyA65 apoprotein from yeast showed a monoexponential assembly kinetics after an initial steep rise, whereas the corresponding apoprotein from *E. coli* showed only a slow monoexponential assembly. The phyB66 apoprotein incorporated either chromophore more slowly than the phyA65s, with biexponential kinetics. With all apoproteins, PΦB was incorporated faster than PCB. The thermal stabilities of the  $P_{fr}$  forms of the N-terminal halves are similar to those known for the full-length recombinant phytochromes: oat phyA65  $P_{fr}$  is highly stable, whereas potato phyB66  $P_{fr}$  is rapidly converted into  $P_r$ . Thus, neither the C-terminal domain nor homodimer formation regulates this property. Rather, it is a characteristic of the phytochrome indicating its origin from mono- or dicots. The  $P_r$  to  $P_{fr}$  kinetics of the N-terminal phyA65 and phyB66 are different. The primary photoproduct  $I_{700}$  of phyA65-PCB decayed monoexponentially and the PΦB analogue biexponentially, whereas the phyB66  $I_{700}$  decayed monoexponentially irrespective of the chromophore incorporated. The formation of  $P_{fr}$  from  $P_r$  is faster with the N-terminal halves than with the full-length phytochromes, indicating an involvement of the C-terminal domain in the relatively slow protein conformational changes.

Higher plants have developed a family of red-light-absorbing photoreceptors, the phytochromes, which regulate a variety of photomorphogenic processes (1, 2). The light-induced physiological function of the phytochromes is based on intimate interactions between the covalently bound chromophore (phytochromobilin, PΦB)<sup>1</sup> and amino acids of the binding site. Thus, a detailed characterization of these interactions is essential for the understanding of the function of phytochromes. Phytochromes exhibit a two-domain structure. The control of the photoisomerization of the chromophore and the guidance of conformational changes of chromophore and protein is a function of the N-terminal half of the protein (3–5), whereas the protein domains involved in signal transduction have been localized in the C-terminal half and in the very first N-terminal 65 amino acids of phytochrome (6, 7).<sup>2</sup>

Former attempts to study the chromophore–protein interactions with chromoprotein fragments obtained by proteolytic digestion of native full-length phytochrome were

impaired by two major problems: (i) only phytochrome A (phyA)-type phytochromes can be prepared in sufficient amounts from etiolated plants, and (ii) in phyA, a simultaneous (and even preferred) proteolysis at position 65 leads to a loss of the front 6 kDa domain of the protein prior to cleavage at position 595 (8).<sup>3</sup> The investigation of such tryptic fragments ( $\Delta 1$ –65,  $\Delta 595$ –1129 = small phytochrome) which lack the terminal 6 kDa portion can lead to confusing results, since these chromopeptides exhibit spectral and kinetic properties different from those of full-length phytochrome, indicating an important role of the first 65 amino acids for the chromophore–protein interactions (3, 9, 10). Heterologous protein expression is a more appropriate strategy since it offers the opportunity of producing chromoprotein fragments of different phytochromes with an intact N-terminal domain and of selectively changed amino acid sequences (11, 12).

Since heterologous expression yields chromophore-free apoproteins, the chromophore–protein interactions during the chromophore assembly as well as the kinetics of the  $P_r \rightarrow P_{fr}$  phototransformation can be studied by using also chromophores other than the native PΦB [e.g., phycocyanobilin (PCB, see Scheme 1)<sup>4</sup> or novel synthetic compounds (13, 14)].

In view of the fact that the control of the photochemical properties of the phytochrome chromophore resides in the

<sup>‡</sup> This article is dedicated to Professor Wolfhart Rüdiger on the occasion of his 65th birthday.

\* To whom correspondence should be addressed.

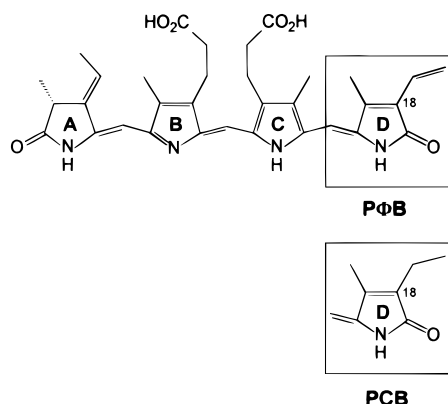
<sup>1</sup> Abbreviations: DMSO, dimethyl sulfoxide; DTT, dithiothreitol; EDTA, ethylenediaminetetraacetic acid; LADS, lifetime-associated difference spectra; PCB, phycocyanobilin; PΦB, phytochromobilin; phyA65-PCB/PΦB, phyB66-PCB/PΦB, N-terminal domain of phytochromes A and B with molecular masses of 65 (oat) and 66 kDa (potato), respectively, carrying either PCB or PΦB as a chromophore.

<sup>2</sup> Note that native phytochromes (i.e., the full-length proteins) exist as dimers, attached at the C-termini, whereas N-terminal fragments (e.g., phyA65) persist as monomers (33).

<sup>3</sup> Numbering of amino acid positions refers to the best characterized phytochrome, phyA from etiolated oat.

<sup>4</sup> For the role of PCB as a biosynthetic precursor of PΦB in algae see Wu et al. (34).

Scheme 1: Formulas of the Tetrapyrroles Phytychromobilin (PΦB) and Phycocyanobilin (PCB)



N-terminal half of the protein, we have used C-terminal truncated recombinant fragments, i.e.,  $\Delta 596$ –1129 oat phyA (apoprotein expressed in *Pichia pastoris* and *Escherichia coli*) and  $\Delta 597$ –1133 potato phyB (expressed in *Saccharomyces cerevisiae*). This report presents first results of a broad investigation aiming at a comparative evaluation of the molecular properties of various phytochromes, such as the in vitro assembly of recombinant apoprotein and chromophore, and the ground state and photochemical events in the phytochrome photocycle (15). It also includes the study of the thermal reversion of  $P_{fr}$  to  $P_r$  in the dark at ambient temperatures, since this process can be considered as a branching pathway in the photocycle. It was practicable at this early stage of the work to first resort to those recombinant phytochromes, the expression and assembly of which were already well established and for which sufficient amounts for spectroscopic studies can be produced. As a consequence, our present comparisons are limited to a juxtaposition of monocot phyA (from oat) and dicot phyB (from potato). The phyA constructs are identical to those recently used in a resonance Raman study (16). The assembly process using PΦB and PCB, the  $P_r \rightarrow P_{fr}$  conversion kinetics in the microsecond-to-second time range as well as the thermal reversion of the  $P_{fr}$  state were studied quantitatively. The investigation of this latter property is of particular interest, since it has been assumed in the literature either to indicate the origin of the phytochromes from monocots or dicots (17, 18) or to depend on the extent of  $P_{fr}$  homodimer generation (17, 19). Lacking the dimerization site located in the C-terminal half, a study of the recombinant N-terminal fragments should help understanding the role of the dimer.

## MATERIALS AND METHODS

**Plasmid Preparation. Generation and Transformation of cDNA Encoding for PhyA65 in *P. pastoris*.** The cDNA encoding the phyA65 peptide was generated from full-length phyA cDNA by PCR with appropriate primers, which introduced *EcoRI* restriction sites directly preceding the ATG codon (5'-end) and following the stop codon at the 3'-end. The stop codon was introduced after the codon for amino acid Arg<sub>595</sub> as described (20). The PCR product was ligated into an *EcoRI*-restricted pHIL-D2 vector (Invitrogen). The resulting plasmid was transformed into competent *P. pastoris* spheroplasts according to the instructions of the manufac-

turer. A cell culture (1 L) was grown for about 1 day to  $A_{600} = 1$ –2 before induction with methanol, as previously described (12).

**Oat PhyA65 Expression in *E. coli*.** For expression in *E. coli*, the plasmid pMEX65KD was used (20), which exhibits an *EcoRI* site in front of the ATG codon and a *SalI* site directly following the stop codon. The stop codon was positioned at identical sites in the plasmids used for the *Pichia* and for the *E. coli* transformation. The expression was performed in the *E. coli* strain C<sub>600</sub> without induction. Cell cultures (1 L) (in TBY, 16 g/L Trypton, 10 g/L yeast extract, 5 g/L NaCl) were grown to a cell density of  $A_{580} = 1.0$  at 37 °C within ca. 4 h.

**Potato PhyB66 Expression in *S. cerevisiae*.** The cDNA encoding the front half of potato phyB was generated by PCR from full-length phyB-cDNA (21). The PCR primers introduced a *BamHI* site at the 5'-end and a stop codon, followed by a *KpnI* site at the 3'-end after nucleotides encoding for amino acid 596. After restriction with *BamHI* and *KpnI* the resulting PCR product was ligated with an appropriately cut p2μG vector (22, 23). This new plasmid was cotransformed with plasmid pG-N795, which encodes the mammalian glucocorticoid receptor, into competent *S. cerevisiae* cells as described recently (21). This cloning allowed for induced expression upon addition of glucocorticoids as reported (22, 23).

**Protein Isolation.** Proteins were isolated in all cases by the same protocol (12). In brief, the harvested cells were disrupted by an Ultra-Turrax at liquid nitrogen temperature. After clarifying the suspensions via ultracentrifugation (100000g, 15 min, 4 °C), the supernatant was kept and the cell pellet was washed once with 100 mM sodium phosphate buffer, pH 7.5 [supplemented with 2 mM of each EDTA, Pefabloc (Merck), and DTT]. The proteins were assembled without further purification with either PCB or PΦB. The amount of recombinant phytochromes was calculated from the absorption spectra using  $\epsilon = 132 \text{ mM}^{-1} \text{ cm}^{-1}$  for all preparations (24). When required, the protein solutions were concentrated with a Centricon 30 cartridge (Amicon).

**Chromophore Incorporation and Generation of Difference Spectra.** Time-resolved chromophore incorporation was performed with highly concentrated solutions of PCB and PΦB (Scheme 1) in DMSO. Both chromophores were prepared and purified by HPLC according to literature (25, 26). After addition to the apoprotein solution, the final chromophore concentration was in each case ca. 10 μM. Concentrations of phytochrome apoproteins were on the order of 0.5 μM, calculated from the difference spectra after complete reconstitution. Consequently, the chromophore was present in 20-fold excess over the protein. The chromoprotein formation was monitored by using a Shimadzu spectrophotometer (UV2102PC), in the dark at 4 and 10 °C for phyA-derived samples and at 4 and 20 °C for phyB-derived samples. Immediately after addition, the absorbance increase at the  $P_r$  maximum (652 nm for PCB and 664 nm for PΦB) was read every 2 s. Due to mixing and handling of the samples, the first data point could only be read ca. 8–10 s after chromophore addition.

For samples with a strong scatter, spectra between 550 and 750 nm were recorded at maximal scanning speed, and the formation rate of  $P_r$  was calculated from the difference spectra. Residual absorption from nonreconstituted chro-

Table 1: Expression Yield and  $P_r$  and  $P_{fr}$  Absorption Maxima (from Difference Spectra) of PhyA and PhyB from the Various Preparations

phytochrome (origin)	yield <sup>a</sup>	incorporated chromophore, $\lambda_{max}$ (nm)			
		PCB		PΦB	
		$P_r$	$P_{fr}$	$P_r$	$P_{fr}$
native phyA124 (oat)				666	730
phyA65 ( <i>P. pastoris</i> )	150 $\mu$ g/L, 20 $\mu$ g/g	653	718	664	729
phyA65 ( <i>E. coli</i> )	50 $\mu$ g/L, 25 $\mu$ g/g	653	715	nd <sup>d</sup>	nd <sup>d</sup>
phyA124 <sup>b</sup> ( <i>P. pastoris</i> )	11 $\mu$ g/g	651	715	663	728
phyB66 ( <i>S. cerevisiae</i> )	35 $\mu$ g/g	658	716	668	726
phyB125 <sup>c</sup> ( <i>S. cerevisiae</i> )	22 $\mu$ g/g	658	714	668	726

<sup>a</sup> The expression yield is calculated in micrograms per liter of cell culture, and in micrograms per gram of cell pellet, on the basis of an absorption coefficient of 132 mM<sup>-1</sup> cm<sup>-1</sup> (24) for all constructs. <sup>b</sup> Data from Schmidt et al. (13). <sup>c</sup> Data from Ruddat et al. (21). <sup>d</sup> nd, not determined.

mophore was taken into account. However, since the absorption coefficients in the long-wavelength range increase by a factor of 13 upon incorporation of the chromophore into the protein, the absorption change of the residual chromophore is negligible. After the assembly was completed, the absorption spectrum was recorded, followed by far-red irradiation in order to determine the state of the assembled chromoprotein in the dark (i.e., formation of  $P_r$  or  $P_{fr}$  forms). Red/far-red irradiation and measurement of difference spectra of completely reconstituted chromoproteins have been described (21).

**Thermal Reversion of the  $P_{fr}$  Forms.** Fully assembled phytochrome fragments were exhaustively irradiated with red light (interference filter,  $\lambda = 659 \pm 10$  nm) and then kept in the dark. The dark reversion to  $P_r$  was followed periodically at ambient temperature (21 °C). The extent of  $P_r$  formation was calculated by measuring absorption spectra at various times or, alternatively, by monitoring the absorption changes at  $\lambda_{max}$  of  $P_r$  continuously.

**Laser-induced Flash Photolysis for Transient Absorbance Measurements.** The experimental setup for flash photolysis was essentially as already described (5, 21). In brief, transient absorbance changes were recorded at 10 °C in the wavelength range 620–740 nm after excitation of the sample with a 650 nm nanosecond pulse from a dye laser, pumped by the second harmonic (532 nm) of a Nd:YAG laser. The excitation pulse ( $<1$  mJ cm<sup>-2</sup>) converted 5–10% of the sample from  $P_r$  to  $P_{fr}$ . In the microsecond time domain, a 700  $\mu$ s time window after the pulse was chosen in order to monitor the  $I_{700}$  decay at wavelengths between 620 and 730 nm. For the  $P_{fr}$  rise kinetics, two time windows of 200 ms and 5 s were chosen at observation wavelengths between 640 and 740 nm. Both series of measurements were combined for data evaluation. Between excitation pulses, the sample was irradiated back to  $P_r$  with far-red light ( $\lambda \geq 730$  nm, two RG9 filters). The collected data were analyzed using a global fit procedure (5, 21) yielding lifetime-associated difference spectra (LADS; Figure 4). It should be kept in mind that in these figures positive amplitudes reflect decay and negative amplitudes growth kinetics, except for the constant which represents the  $P_{fr}$  minus  $P_r$  difference spectrum.

## RESULTS

**Heterologous Expression.** Both oat phyA65 and potato phyB66 apoproteins were obtained in greater yield than the full-length apoproteins. For the yeast-derived recombinant phytochromes, the 65 kDa domain was expressed in about

twice the amount as the full-length protein (see Table 1). When comparing the amount of protein with respect to the expression systems, the yield per gram of cell pellet was in the same range for *E. coli* and for *P. pastoris* (Table 1, 25 and 20  $\mu$ g/g, respectively), but the cell pellet weight obtained from the *E. coli* cell cultures was less than one-third of that from *P. pastoris* (2 g vs 7.5 g). In view of a literature report on an endogenous production of PΦB by *P. pastoris* (27), which can lead to holoprotein formation already during cell growth, we have scavenged our apoprotein preparations for the presence of holoprotein by absorption difference spectroscopy. Under the growth conditions used (white light irradiation), the amounts of endogenously formed holophytochromes always were less than 10% assembled in vitro. Such number is too low to critically interfere with the interpretation of our data.

The yield of expressed potato phyB66 was 1.6 times that of full-length apoprotein (35  $\mu$ g/g cell pellet vs 22  $\mu$ g/g). Since both yeast expression systems (*P. pastoris* and *S. cerevisiae*) yielded similar amounts of apoprotein [as determined for the full-length apoprotein (21)], expression of phyB66 was carried out in *S. cerevisiae* for reasons of convenience.

**$P_r$  and  $P_{fr}$  Absorption Maxima.** The phyA65-PΦB fragment (from yeast expression) absorbs at 664 and 729 nm ( $P_r$  and  $P_{fr}$ , respectively), and phyA65-PCB at 653 and 718 nm. The  $P_r$  maximum of phyA65-PCB from bacterial expression is the same as that of the yeast-derived protein (653 nm), while the  $P_{fr}$  maximum is slightly blue shifted to 715 nm. The maxima of phyB66-PΦB are at 668 and 726 nm ( $P_r$  and  $P_{fr}$ , respectively), and those of phyB66-PCB at 658 and 716 nm, respectively (see Table 1). All values were determined from the difference spectra.

**Chromophore Assembly Kinetics.** Covalent binding of the chromophore causes a red absorption shift and a marked increase of absorbance. Since assembly in the dark exclusively produces the  $P_r$  form of the recombinant phytochrome (see below), the incorporation can be monitored in a quantitative manner at 664 (PΦB) and 652 nm (PCB). Whereas the phyB incorporation kinetics is slower than that of phyA and could thus be followed at 20 °C, the assembly of the phyA apoprotein had to be determined at lower temperatures (4 and 10 °C).

**65 kDa PhyA Protein from Oat.** Interestingly, the assembly kinetics of the apoproteins from *E. coli* and yeast are different. The data of *E. coli* derived apoprotein and PCB could be fitted with a monoexponential kinetics with a lifetime ( $\tau_{obs}$ ) of 500 s (at 4 °C), decreasing to 280 s at 10



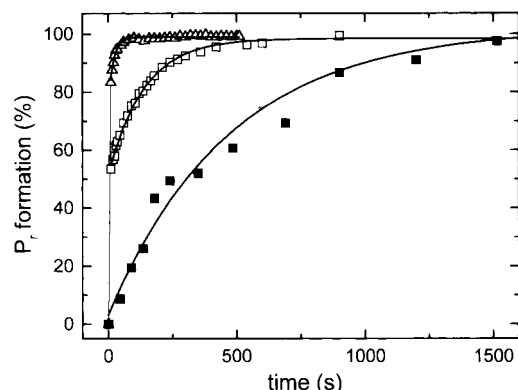


FIGURE 1: Assembly kinetics of phyA65 apoprotein. Absorbance of  $P_r$ , expressed as percent of maximal value upon incubation of phyA65 apoprotein (from bacterial or yeast expression) with PΦB (monitored at 664 nm) and PCB (monitored at 652 nm, both at 4 °C). (■) *E. coli* derived apoprotein + PCB, and yeast-derived apoprotein + (□) PCB and (Δ) PΦB.

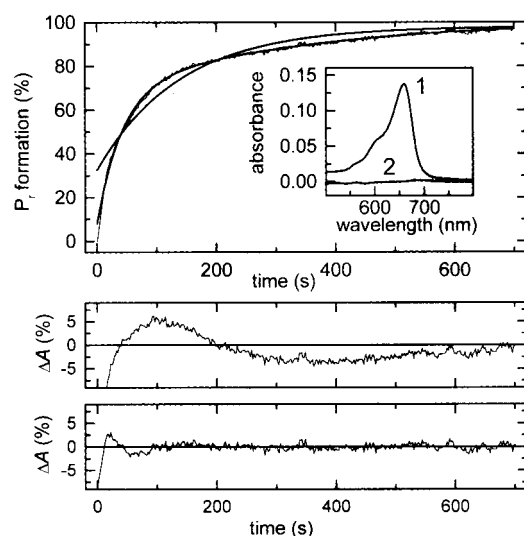


FIGURE 2: (Top) Assembly kinetics of phyB66 apoprotein. Absorbance of  $P_r$ , expressed as percent of maximal value upon incubation of phyB66 apoprotein with PCB (at 4 °C). The absorption rise at around 660 nm fits to a biexponential kinetics and clearly deviates from a monoexponential function (also shown for demonstration). (Bottom) Plots of residuals between data points and fitting curves (upper residuals, monoexponential fit; lower residuals, biexponential fit). The inset shows the final absorption spectrum of the phytochrome ( $P_r$ ) formed (trace 1). To demonstrate the exclusive formation of the  $P_r$  state in the assembly process, the reconstituted sample was irradiated with far-red light. The difference between both spectra gave a flat line (trace 2).

°C, whereas for the yeast-derived apoprotein and PCB, a value of  $\tau_{\text{obs}} = 137$  s (4 °C) was determined (Figure 1 and Table 2).

PΦB led to a remarkable acceleration of the assembly ( $\tau_{\text{obs}} = 20$  s, Table 2). Comparison of the assembly kinetics reveals that the absorbance of the *E. coli* derived apoprotein grows gradually, starting with the first data point at  $\Delta A = 0$ , whereas already the first data points of the yeast-derived apoprotein exhibit a strong offset which comprises between 50% (PCB) and 80% (PΦB) of the total absorbance increase. This indicates a much faster process preceding the relatively slow subsequent kinetics. For this reason, the first data point (at zero time) was omitted for the calculation of the assembly rate. In all cases, the inspection of the residuals reveals that the first 20 s of the assembly are disturbed most probably

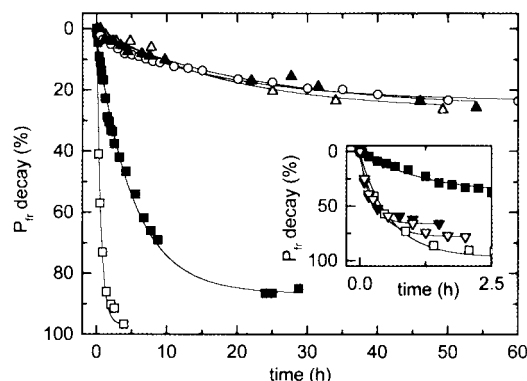


FIGURE 3: Thermal instability of the  $P_{fr}$  forms (i.e., their reversal to  $P_r$  in the dark) of various native and recombinant phytochromes, monitored at  $\lambda_{\text{max}}$ . (○) Native full-length oat phyA (124 kDa;  $\lambda_{\text{max}} = 730$  nm; data from ref 5), (Δ) phyA65-PΦB ( $\lambda_{\text{max}} = 729$  nm), (▲) phyA65-PCB ( $\lambda_{\text{max}} = 718$  nm), (□) phyB66-PΦB ( $\lambda_{\text{max}} = 726$  nm), (■) phyB66-PCB ( $\lambda_{\text{max}} = 716$  nm). The inset shows the time course of  $P_{fr}$  reversion for the phyB-related chromoproteins during the first 2.5 h. For comparison, the data from the phyB full-length recombinant protein (from ref 21) has been included: (▽) phyB-PΦB ( $\lambda_{\text{max}} = 726$  nm); (▼) phyB-PCB ( $\lambda_{\text{max}} = 714$  nm). PhyA65 apoproteins were expressed in *P. pastoris*, and all phyB apoproteins in *S. cerevisiae*.

due to the mixing process in the cuvette.

**66 kDa PhyB Protein from Potato.** The assembly is clearly biphasic for phyB66, with both lifetimes in the range of seconds (Figure 2 and Table 2). Attempts to fit the experimental data with a single-exponential growth, irrespective of whether PΦB or PCB was used as a chromophore, led to significant deviations (upper residuals in Figure 2). Monitoring the increase at the respective  $\lambda_{\text{max}}$  yielded two lifetimes of  $\tau_{\text{obs}} = 9$  and 83 s for PΦB, and of  $\tau_{\text{obs}} = 17$  and 147 s for PCB ( $T = 20$  °C, Table 2). Again, the incorporation of the native chromophore (PΦB) was faster than that of PCB. To allow for a comparison with the phyA65 chromoprotein, the assembly with PCB was also monitored at 4 °C and afforded  $\tau_{\text{obs}}$  of 40 and 340 s.

No changes in these kinetic parameters were observed when the amount of PCB was varied between a 10- and 30-fold excess (data not shown). The absorption spectra, recorded after the completion of the assembly, were identical to those obtained upon subsequent saturating far-red irradiation, which indicates that the  $P_r$  form of phytochrome was exclusively generated (inset in Figure 2). A zinc blot clearly showed the fluorescence of the protein-bound chromophore comigrating with the peptide band in the SDS-electrophoresis gel (data not shown) confirming that a covalent bond between chromophore and protein had been formed in the assembly process.

**Thermal Reversion of the  $P_{fr}$  Forms.** Fully assembled PΦB- and PCB-containing phyA65 and phyB66 holoproteins were exhaustively irradiated at ambient temperature with red light of 659 nm to achieve maximal transformation to  $P_{fr}$ . The samples were kept in the dark for up to 50 h during which spectra were measured.

Figure 3 shows the  $P_{fr}$  thermal reversions at ambient temperature of the phyA65 and phyB66 constructs, assembled with PCB and PΦB. For comparison, the thermal reversions of the full-length native oat phyA and of the recombinant potato phyB phytochrome are also shown (from refs 5 and 21). The phyA65 fragments (with either chro-

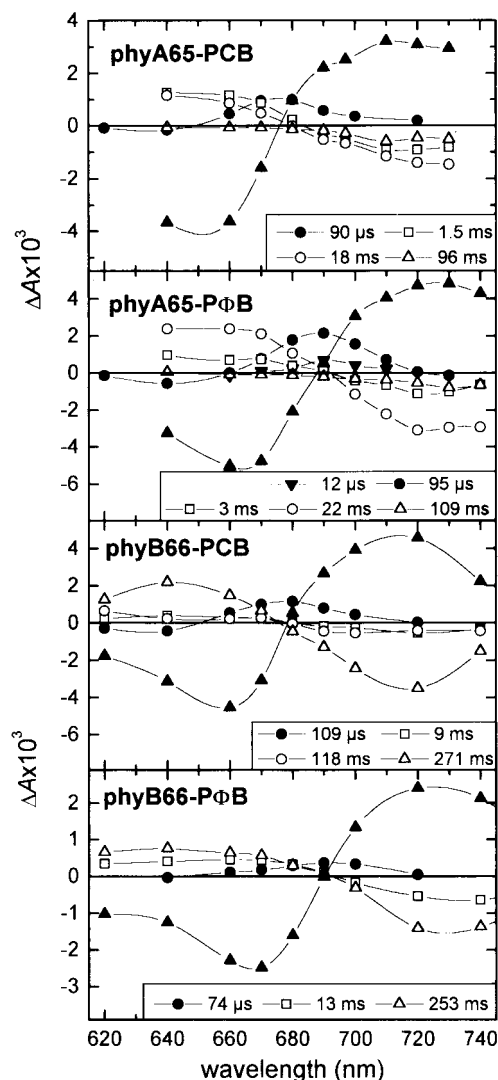


FIGURE 4: Lifetime-associated difference spectra (LADS) of  $I_{700}$  decay and  $P_{fr}$  rise determined by ns flash photolysis; ( $\blacktriangle$ ) constant term [ $=\Delta(P_{fr} - P_r)$ ]. (Top) In oat phyA65-PCB and phyA65-P $\Phi$ B. Apoproteins expressed in *P. pastoris*. (Bottom) In potato phyB66-PCB and phyB66-P $\Phi$ B. Apoproteins expressed in *S. cerevisiae*. mophore) are as stable as native oat phytochrome. They reverted back to  $P_r$  by only 25% within 50 h.

In contrast, all phyB66-related chromoproteins undergo a much more rapid reversion to  $P_r$ . Whereas 80% of the initial  $P_{fr}$  of the PCB chromoprotein had reverted back into  $P_r$  only after 13 h, the P $\Phi$ B-containing chromoprotein showed the same extent of conversion (80%) already after ca. 1 h. Interestingly, this difference in behavior is not as pronounced in the full-length phyB recombinant proteins (see inset in Figure 3).

Loss of covalently bound chromophore was not detected even after 50 h, since the phytochromes are fully photo-reversible with same amounts of  $P_r$  and  $P_{fr}$  as in the beginning of the experiment.

**Flash Photolysis.** (a) *Oat PhyA65 Fragments: The  $I_{700}$  Decay.* The absorbance at around 700 nm (indicative of the first photointermediate,  $I_{700}$ ) of phyA65-P $\Phi$ B decayed biexponentially ( $\tau_1 = 12 \mu\text{s}$ ,  $\tau_2 = 95 \mu\text{s}$ ; Figure 4), whereas the PCB-containing fragment decayed monoexponentially, irrespective of the expression system ( $\tau = 75 \mu\text{s}$  for the protein from *E. coli* and  $\tau = 90 \mu\text{s}$  for that from *P. pastoris*; Figure 4 and Table 3).

(b) *Oat PhyA65 Fragments: The  $P_{fr}$  Rise.* For both expression systems (*E. coli* and *P. pastoris*) and for both chromophores, the rise in the far-red region (i.e., the measure of the  $P_{fr}$  formation) could be fitted with three kinetic components. PCB-containing samples showed similar lifetimes of (values for *E. coli*-derived proteins given in parentheses) 1.5 (1.5), 18 (14), and 96 (80) ms (Figure 4). The sample with P $\Phi$ B (only prepared with yeast-derived apoprotein) also showed three lifetimes of 3, 22, and 109 ms. For both expression systems, the second component exhibited the largest amplitude, a bleaching at around 670 nm, and a concomitant absorbance increase at around 720–730 nm. The slowest process (with a lifetime around 100 ms) did not show any spectral changes in the short-wavelength region and only exhibited a small increase in the  $P_{fr}$  absorption range.

(c) *Potato PhyB66: The  $I_{700}$  Decay.* The comparison of full-length potato phyB with full-length oat phyA (21) reveals a significant difference for the  $I_{700}$  decay such that in phyB—irrespective of the chromophore used—a monoexponential decay was observed (compare data in Table 3 for phyA-P $\Phi$ B). The same situation holds true for the N-terminal halves of both phytochromes (Figure 4): the phyB66-proteins decayed monoexponentially with  $\tau = 74 \mu\text{s}$  (phyB66-P $\Phi$ B) and  $\tau = 109 \mu\text{s}$  (phyB66-PCB).

(d) *Potato PhyB66: The  $P_{fr}$  Rise.* The  $P_{fr}$  rise is clearly slower for phyB66 than for phyA65. The rise for phyB66-PCB was best fitted with three time constants of  $\tau_1 = 9$ ,  $\tau_2 = 118$ , and  $\tau_3 = 271$  ms, whereas for the P $\Phi$ B fragment, two components with  $\tau_1 = 13$  and  $\tau_2 = 253$  ms were sufficient for a good fit (Figure 4 and Table 3). The growth lifetime of 13 ms of phyB66-P $\Phi$ B is relatively close to the 9 ms component of the PCB sample. Any component of about 100 ms—if at all present as in the PCB sample—should exhibit a very small amplitude only.

## DISCUSSION

**Expression of Apoprotein.** A comparison of the expression yield with reported data (12, 21) reveals that in all cases the N-terminal halves are obtained in larger amounts than the corresponding full-length apoproteins. This might be due to the relatively large size of the latter, which makes an efficient synthesis and correct folding of the apoprotein a more difficult task for the biosynthetic apparatus of the host cell. Moreover, the stability toward degradation may critically depend on the perfection of the folding. The former hypothesis is supported by Kunkel et al. (28) who report a higher yield of recombinant phytochrome upon expression in yeast when the chromophore has been introduced into the host cell.

**$P_r$  and  $P_{fr}$  Absorption Maxima.** Whereas the various hosts produce different amounts of protein which, in addition, differ in their assembly kinetics, the difference absorption maxima and  $P_r \rightarrow P_{fr}$  kinetics of both the *E. coli* derived and the yeast-derived chromoproteins are the same. The difference absorption maxima are very close to those of the full-length proteins. This again emphasizes the dominant role of the N-terminal half in the regulation of the spectral properties. Interestingly, the phyB-related chromoproteins—when compared to phyA—exhibit a red shift of the  $P_r$  absorption maximum whereas the  $P_{fr}$  maximum is nearly

Table 2: Parameters of Assembly Kinetics for PhyA65 and PhyB66<sup>a</sup>

phytochrome (origin)	temp (°C)	PCB assembly $\tau_{\text{obs}} [s]/(k [s^{-1}])$	PΦB assembly $\tau_{\text{obs}} [s]/(k [s^{-1}])$
phyA65 ( <i>P. pastoris</i> )	4	137/(7.3 × 10 <sup>-3</sup> ) <sup>b</sup>	20/(5 × 10 <sup>-2</sup> ) <sup>b</sup>
phyA65 ( <i>E. coli</i> )	4	500/(2 × 10 <sup>-3</sup> )	nd <sup>c</sup>
	10	280/(3.6 × 10 <sup>-3</sup> )	
phyB66	4	40/(2.5 × 10 <sup>-2</sup> ), 340/(2.9 × 10 <sup>-3</sup> )	nd <sup>c</sup>
( <i>S. cerevisiae</i> )	20	17/(5.8 × 10 <sup>-2</sup> ), 147/(6.8 × 10 <sup>-3</sup> )	9/(11 × 10 <sup>-2</sup> ), 83/(12 × 10 <sup>-3</sup> )

<sup>a</sup> P<sub>r</sub> formation, measured at 652 (PCB) and 664 nm (PΦB). <sup>b</sup> This assembly is biphasic, with an unresolved fast component (see text for further details). <sup>c</sup> nd, not determined.

Table 3: P<sub>r</sub> → P<sub>fr</sub> Photoconversion: Lifetimes of I<sub>700</sub> Decay and P<sub>fr</sub> Formation

phytochrome (origin)	lifetimes of the I <sub>700</sub> decay		lifetimes of the P <sub>fr</sub> rise		
	$\tau_1$ (μs)	$\tau_2$ (μs)	$\tau_1$ (ms)	$\tau_2$ (ms)	$\tau_3$ (ms)
phyA65-PΦB ( <i>P. pastoris</i> )	12	95	3	22	109
phyA65-PCB ( <i>P. pastoris</i> )		90	1.5	18	96
phyA65-PCB ( <i>E. coli</i> )		75	1.5	14	80
native phyA124 (oat) <sup>a</sup>	11.5	85	6.7	50	427, 3020
phyA124-PΦB ( <i>P. pastoris</i> ) <sup>a</sup>	10	90	3.8	25	164, 2570
phyB66-PΦB ( <i>S. cerevisiae</i> )		74	13		253
phyB66-PCB ( <i>S. cerevisiae</i> )		109	9	118	271
phyB125-PΦB ( <i>S. cerevisiae</i> ) <sup>b</sup>		85		23	345, 2080 <sup>c</sup>
phyB125-PCB ( <i>S. cerevisiae</i> ) <sup>b</sup>		85		8	125, 730

<sup>a</sup> Data from Schmidt et al. (5). <sup>b</sup> Data from Ruddat et al. (21). <sup>c</sup> Note that this kinetic process refers to a P<sub>fr</sub> → P<sub>r</sub> thermal reversion; for detailed discussion, see Ruddat et al. (21).

identical. This observation is in contrast to the recently reported blue-shifted P<sub>fr</sub> absorption for recombinant phyB from tobacco [ $\lambda_{\text{max}} = 712$  nm (29)].

**Chromoprotein Assembly Kinetics.** The substitution of the native PΦB chromophore with PCB in full-length oat phyA leads to a marked decrease of the rate constants of chromoprotein reconstitution (30) and to significant changes in the characteristics of the decay kinetics of the first intermediate, I<sub>700</sub>, in the P<sub>r</sub> → P<sub>fr</sub> phototransformation (ref 13; see below). Since the two chromophores differ only in the ring D substituent at C-18, these differences reveal a specific interaction between the protein-binding site and this particular chromophore substituent (vinyl in PΦB and ethyl in PCB; Scheme 1). Accordingly, we now find a similarly faster assembly with PΦB than with PCB for the oat phyA65 and potato phyB66 apoprotein fragments. Moreover, the assembly kinetics of the two proteins are quite different as well. We find an instantaneous rise of the phyA P<sub>r</sub> absorption, followed by a slower process (20 s for PΦB and 137 s for PCB). The phyB66 assembly is also biphasic. However, the first rapid rise, not resolved in phyA65, is considerably slower here and directly observable on the time scale of seconds (Table 2).

Li and Lagarias (30) have interpreted the two-step assembly process as follows: (i) the formation of an intermediate with the chromophore not covalently attached to the protein, followed by (ii) a catalytic formation of the covalent bond between chromophore and protein. In process i, the affinity of the apoprotein for the chromophore supposedly requires a particular conformation of the binding site capable of a specific recognition of the chromophore. This conformational prerequisite does not seem to be fulfilled with the phyA65 apoprotein from *E. coli*. In this case, the PCB assembly kinetics is monoexponential with a slow growth of the absorbance ( $\tau_{\text{obs}} = 500$  s at 4 °C, Table 2), starting at  $\Delta A = 0$  without an instantaneous rise at the beginning of

the reconstitution. Obviously, the folding of the polypeptide chain in bacteria is imperfect and does not allow for a rapid complex formation between chromophore and protein.

Differences between bacterial- and yeast-expressed apoproteins have also been found for the chromoprotein assembly employing oat phyA39 apoprotein [amino acids 65–425 (12)]. Here, P<sub>r</sub> and P<sub>fr</sub> forms could be obtained with the yeast-derived apoprotein, whereas the corresponding polypeptide from bacterial expression had lost the capability to assemble the chromophore.

Assembly of chromoproteins from recombinant phytochrome apoproteins has been reported by several other groups. Since various detection methods for phytochrome formation have been employed, a comparison of results is difficult. In most cases, the chromophore was added in great excess, turning the assembly kinetics into pseudo-first order. Li and Lagarias (30) reported binding of PΦB to phyA apoprotein to be faster than with PCB by a factor of 2 (2.1 × 10<sup>-2</sup> s<sup>-1</sup> vs 9.8 × 10<sup>-3</sup> s<sup>-1</sup>, both at 0 °C), whereas we find an acceleration factor as large as 7. The  $k$  value determined in this study (7.3 × 10<sup>-3</sup> s<sup>-1</sup>) for PCB is similar to that found by others (11, 30) (7.8 × 10<sup>-3</sup> s<sup>-1</sup>), although the latter value was determined for recombinant phyA from pea (all values at 4 °C). Interestingly, also the binding of PCB to tobacco phyB apoprotein is in the same order of magnitude (2.8 × 10<sup>-2</sup> s<sup>-1</sup>), irrespective of the excess in chromophore varying from 30- to 140-fold (28). In contrast, the data presented here clearly show a biphasic kinetics for phyB66 with the first lifetime in the same range as the value reported for tobacco phyB (28), but revealing an additional, formerly not described slow component with  $\tau_{\text{obs}}$  of ca. 6 min.

**Thermal P<sub>fr</sub> → P<sub>r</sub> Reversion.** Vierstra (18) has reported that the P<sub>fr</sub> state of phytochrome from monocots is more stable than that from dicots, which in general shows a rapid thermal backreaction to P<sub>r</sub>. The physiological significance



of this thermal  $P_{fr} \rightarrow P_r$  reversion is not yet understood in detail. It was suggested that this process competes in vivo with enzymatic degradation and thus could have a special significance under daylight conditions. For a discussion of this proposal, one should keep in mind that no phyB from a monocot has yet been isolated in pure form, although Tokuhisha et al. (31) described a thermally stable phytochrome in deetiolated oat, which can be assumed to be of phyB type. This result might justify the just-mentioned possibility that stability/reversion depends on the origin of the phytochrome, i.e., from either mono- or dicot plants. A contradiction to this discussion is the report by Kunkel et al. (28) about the high  $P_{fr}$  stability of recombinant rice phyA and tobacco phyB in living yeast cells, from which one may conclude that stability/reversion is probably not an endogenous property of the particular phytochrome, but rather is regulated by yet unidentified components of the plant. Considering these various possibilities for the in vivo  $P_{fr}$  stability, i.e., either being an effect of greater intrinsic stability or being due to de novo synthesis of the protein compensating for the degradation, our in vitro results support the proposal that in general phytochromes from monocots seem to be more stable than phytochromes from dicots: recombinant phyB  $P_{fr}$  (125 and 66 kDa proteins) and also full-length phyA  $P_{fr}$  of the dicot potato (21) revert within a short time almost completely to the  $P_r$  form, whereas phyA chromoproteins of oat are stable for days (see also ref 5). Again, a distinct protein-chromophore interaction is apparently responsible for the regulation of this reaction. Monitoring the reversion at various temperatures allows a calculation of the energy barriers for this thermal process. A detailed analysis is currently performed.

$P_r \rightarrow P_{fr}$  Photoconversion. While the chromophore assembly kinetics of phyA65 depends markedly on the expression system, no such effect could be observed on the  $P_r \rightarrow P_{fr}$  phototransformation. A difference was not expected a priori, since any conformational inadequacies of the protein-binding pocket should be rectified in the course of assembly step i (see above). The chromophore-induced protein conformational change is also in line with the circular dichroism evidence by Furuya and Song (32), which reveals that apo- and holoprotein possess different secondary structures.

The specific interaction of the C-18 substituent with the surrounding protein determines the  $I_{700}$  decay kinetics, which is biexponential in the case of phyA65-P $\Phi$ B and monoexponential in the case of phyA65-PCB (Table 3). The decay lifetime component of around 90  $\mu$ s is not affected noticeably by either protein length or chromophore type. This result concurs with recent resonance Raman studies on the N-terminal half of phyA, carrying either of the two chromophores, which have shown strong conformational similarities between the protein-bound P $\Phi$ B and PCB molecules (16).

For both chromoproteins, the kinetics of the  $P_{fr}$  rise are in the millisecond time range (Figure 4). However, the phyB66-PCB transforms slower by a factor of ca. 2.7 than phyA65-PCB. The detection of only two components in the case of phyB66-P $\Phi$ B might reflect a problem of resolution. Should this component be present, it would have a very small amplitude. Comparison of the  $P_{fr}$  growth rate of the N-terminal fragments with the full-length proteins reveals

that in every case the C-terminus slows down the transformation.

Another difference between phyA and phyB becomes obvious in the amplitudes of the millisecond LADS. The first two  $P_{fr}$  rise components for phyA65 (e.g., 1.5 and 18 ms for phyA65-PCB)—independent of the expression system and the chromophore used—have the largest amplitudes, whereas the longest-lived one (96 ms) has no contribution in the red and only a very small amplitude in the far-red region. The spectral appearance of this component is already quite similar to  $P_{fr}$ . In contrast, the  $P_{fr}$  rise kinetics for phyB66-PCB has a large amplitude for the longest lifetime, as already observed for full-length potato phyB (21), indicating that in phyB the typical  $P_{fr}$ -like spectral shape is generated during the very last kinetic step. It is thus concluded that  $P_{fr}$  formation is significantly different in phyA and phyB (Figure 4 and Table 3).

It is interesting to speculate that these differences in the  $P_{fr}$  rise kinetics (in the hundreds of milliseconds) between phyA and phyB as well as between full-length phytochromes and the N-terminal halves are a requirement for signal transduction.

## CONCLUSION

Differences in the kinetics of chromophore assembly are attributed to the variable influence on the apophytochrome folding by the expression system chosen. Once the chromophore is bound, the protein adopts its final conformation, so that no differences in the photochemistry are detectable irrespective of the expression system.

The thermal  $P_{fr}$  stability in vitro is independent of the C-terminal part of the protein, which excludes a mechanism that involves phytochrome dimers.

The C-terminus of phytochrome increases the reaction time of the  $P_{fr}$  formation, which suggests an involvement of extensive protein rearrangements. The kinetics of  $P_{fr}$  formation also depend on the type of phytochrome (compare the reactions of phyA65 and phyB66).

## ACKNOWLEDGMENT

Antibodies for Western blots were kindly provided by Prof. Brian Thomas and Dr. Michael Partis, Warwick, U.K. (phyA), and by Prof. Peter H. Quail, Albany, CA (phyB). The assistance of Peter Schmidt in the flash photolysis measurements is gratefully acknowledged, as is the technical help of Gül Koc and Tanja Berndsen in chromophore preparation and purification.

## REFERENCES

1. Kendrick, R. E., and Kronenberg, G. H. M., Eds. (1994) *Photomorphogenesis in Plants*, Kluwer Academic Publishers, Dordrecht, Netherlands.
2. Smith, H., Ed. (1997) *Plant Cell Environ.* 20, 657–844 (special issue).
3. Ruzsicska, B. P., Braslavsky, S. E., and Schaffner, K. (1985) *Photochem. Photobiol.* 41, 681.
4. Mozley, D., Remberg, A., and Gärtner, W. (1997) *Photochem. Photobiol.* 66, 710.
5. Schmidt, P., Gensch, T., Remberg, A., Gärtner, W., Braslavsky, S. E., and Schaffner, K. (1998) *Photochem. Photobiol.* In press.
6. Cherry, J. R., Hondred, D., Walker, J. M., and Vierstra, R. D. (1992) *Proc. Natl. Acad. Sci. U.S.A.* 89, 5039.

7. Quail, P. H., Boylan, M. T., Parks, B. M., Short, T. W., Xu, Y., and Wagner, D. (1995) *Science* 268, 675.
8. Grimm, R., Lottspeich, F., Schneider-Poetsch, H. A. W., and Rüdiger, W. (1986) *Z. Naturforsch.* 41C, 993.
9. Farrens, D., Cordonnier, M.-M., Pratt, L. H., and Song, P.-S. (1992) *Photochem. Photobiol.* 56, 725.
10. Jordan, E. T., Cherry, J. R., Walker, J. M., and Vierstra, R. D. (1995) *Plant J.* 9, 243.
11. Deforce, L., Furuya, M., and Song, P.-S. (1993) *Biochemistry* 32, 14165.
12. Gärtner, W., Hill, C., Worm, K., Braslavsky, S. E., and Schaffner, K. (1996) *Eur. J. Biochem.* 236, 978.
13. Schmidt, P., Westphal, U. H., Worm, K., Braslavsky, S. E., Gärtner, W., and Schaffner, K. (1996) *J. Photochem. Photobiol. B* 34, 73.
14. Lindner, I., Gärtner, W., Braslavsky, S. E., and Schaffner, K. (1998) *Angew. Chem.* (In press).
15. Matysik, J., Hildebrandt, P., Schlamann, W., Braslavsky, S. E., and Schaffner, K. (1995) *Biochemistry* 34, 10497.
16. Kneip, C., Mozley, D., Hildebrandt, P., Gärtner, W., Braslavsky, S. E., and Schaffner, K. (1997) *FEBS Lett.* 414, 23.
17. Mancinelli, A. L. (1993) in *Photomorphogenesis in Plants*, 2nd ed. (Kendrick, R. E., and Kronenberg, G. H. M., Eds.) pp 211–269, Kluwer Academic Publishers, Dordrecht, Netherlands.
18. Vierstra, R. D. (1993) in *Photomorphogenesis in plants*, 2nd ed. (Kendrick, R. E., and Kronenberg, G. H. M., Eds.) pp 141–160, Kluwer Academic Publishers, Dordrecht, Netherlands.
19. Furuya, M., and Schäfer, E. (1996) *Trends Plant Sci.* 1, 301.
20. Hill, C., Gärtner, W., Townner, P., Braslavsky, S. E., and Schaffner, K. (1994) *Eur. J. Biochem.* 223, 69.
21. Ruddat, A., Schmidt, P., Gatz, C., Braslavsky, S. E., Gärtner, W., and Schaffner, K. (1997) *Biochemistry* 36, 103.
22. Schena, M., and Yamamoto, K. R. (1988) *Science* 241, 965.
23. Picard, D., Schena, M., and Yamamoto, K. R. (1990) *Gene* 86, 257.
24. Lagarias, J. C., Kelly, J. M., Cyr, K. L., and Smith, J. W. O. (1987) *Photochem. Photobiol.* 46, 5.
25. Kufer, W., and Scheer, H. (1979) *Hoppe-Seyler's Z. Physiol. Chem.* 360, 935.
26. Cornejo, J., Beale, S. I., Terry, M. J., and Lagarias, J. C. (1992) *J. Biol. Chem.* 267, 14790.
27. Wu, S.-H., and Lagarias, J. C. (1996) *Proc. Natl. Acad. Sci. U.S.A.* 93, 8989.
28. Kunkel, T., Speth, V., Büche, C., and Schäfer, E. (1995) *J. Biol. Chem.* 270, 20193.
29. Kunkel, T., Tomizawa, K.-I., Kern, R., Furuya, M., Chua, N.-H., and Schäfer, E. (1993) *Eur. J. Biochem.* 215, 587.
30. Li, L., and Lagarias, J. C. (1992) *J. Biol. Chem.* 267, 19204.
31. Tokuhisha, G., Daniels, S. M., and Quail, P. H. (1985) *Planta* 164, 321.
32. Furuya, M., and Song, P.-S. (1993) in *Photomorphogenesis in Plants*, 2nd ed. (Kendrick, R. E., and Kronenberg, G. H. M., Eds.) pp 105–140, Kluwer Academic Publishers, Dordrecht, Netherlands.
33. Cherry, J. R., Hondred, D., Walker, J. M., Keller, J. M., Hershey, H. P., and Vierstra, R. D. (1993) *Plant Cell* 5, 565.
34. Wu, S.-H., McDowell, M. T., and Lagarias, J. C. (1997) *J. Biol. Chem.* 272, 25700.

BI980575X